Lasers in Manufacturing Conference 2021

Emission of X-rays during ultrashort pulse laser processing

Herbert Legall[a], Jörn Bonse[a], Jörg Krüger[a,*]

[a]*Bundesanstalt für Materialforschung und -prüfung (BAM), Unter den Eichen 87, 12205 Berlin, Germany*

Abstract

Ultrashort pulse laser materials processing can be accompanied by the production of X-rays. Small doses per laser pulse can accumulate to significant dose rates at high laser pulse repetition rates which may exceed the permitted X-ray limits for human exposure. Consequently, a proper radiation shielding must be considered in laser machining. A brief overview of the current state of the art in the field of undesired generation of X-ray radiation during ultrashort pulse laser material processing in air is presented.

Keywords: ultra-short pulse laser processing; laser-induced X-ray emission; radiation protection

1. Introduction

The use of ultrashort laser pulses in laser materials processing has left the niche and is becoming more and more established in industrial practice. In addition to the physical advantages of using ultrashort pulse durations, high average laser powers combined with high pulse repetition rates increasingly allow economically viable application. However, as a result of the single pulse laser – matter interaction in air, hazardous X-ray radiation can be generated and can accumulate to dose levels above the X-ray limits for human exposure due to high pulse repetition rates. Recently, a review paper was published summarizing the state of the art in the field of undesired generation of X-ray radiation during ultrashort pulse laser processing in air (Legall et al., 2021). Here, some important facts regarding the measured X-ray doses, X-ray spectra, and radiation protection shielding are presented.

* Corresponding author. Tel.: +49-30-8104-1822; fax: +49-30-8104-71822
E-mail address: joerg.krueger@bam.de

2. X-ray generation

A scheme of the X-ray generation process is depicted in Fig. 1. If an ultrashort laser pulse with an intensity above the ablation threshold hits a workpiece, a near-surface electron plasma is generated via absorption and ionization of the material ("plasma generation", left). The laser pulse energy is transferred to the plasma electrons by laser-plasma interactions ("plasma heating", middle). As a result of the interplay of these "hot" plasma electrons with the workpiece, spectrally continuous Bremsstrahlung and characteristic X-ray radiation can be produced ("X-ray emission", right). The laser-based generation process of the X-rays is similar to that in a conventional X-ray tube, but there is no cut-off X-ray energy limited by the accelerating voltage of the X-ray tube. The Maxwellian-shaped energetic distribution of the "hot" plasma electrons determines the spectral distribution of the emitted X-ray radiation.

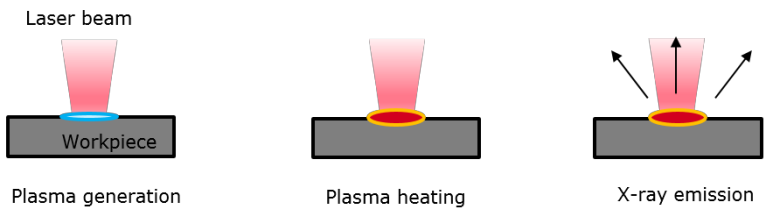

Fig. 1. Scheme of X-ray-generation. Firstly, a plasma is generated via ionization (left). Energy is transferred from the laser beam to the plasma electrons, heating them up (middle). X-ray radiation can be generated by interaction of the "hot" plasma electrons with the plasma ions during laser material processing (right). Adapted from Legall et al., 2019a.

3. X-ray doses

For the measurement of pulsed X-ray radiation doses *passive* X-ray dose storing systems as e.g. thermo luminescence dosimeters (TLD) are recommended to avoid an underestimation of the doses (Alves et al., 2011). The disadvantage of passive dosimeters is the need for manual readout after each exposure, which is not convenient for the alignment of a radiation source or if measurements must be repeated many times. In these cases, *active* dosimeters (e.g. ionization chambers) are more appropriate. It was demonstrated by the simultaneous use of active and passive dosimeters that under certain conditions an active dosimeter can be used for the reliable determination of X-ray doses (Legall et al., 2018).

For the 925-fs laser treatment of tungsten at 1030 nm wavelength and 400 kHz repetition rate, X-ray skin dose rates up to $\dot{H}'(0.07)$ = 163 mSv/h were measured in a distance of 420 mm from the laser interaction zone, when employing a laser peak intensity of 2.6×10^{14} W/cm^2. Maximum averaged X-ray skin doses per pulse $H'(0.07) \sim 0.1$ nSv are found. This means that the annual skin dose radiation limit for members of the public of $H'(0.07)$ = 50 mSv can be reached in less than one hour in a distance of 420 mm from the laser interaction zone without protection shielding (Legall et al., 2018).

At a smaller distance of 10 cm from the laser ablation spot, the situation is even more critical. For the laser parameters given above and tungsten as workpiece, skin dose rates of $\dot{H}'(0.07)$ = 10.8 Sv/h were then calculated (Legall et al., 2018). These results were confirmed by Behrens et al., 2019, reporting skin dose rates of $\dot{H}'(0.07)$ = 4.8 Sv/h for tungsten and $\dot{H}'(0.07)$ = 8.3 Sv/h for a tungsten alloy using a laser peak intensity of 2.1×10^{14} W/cm^2 and a pulse duration of 924 fs, a wavelength of 1030 nm, and 400 kHz repetition rate.

The atomic number of the workpiece Z plays a decisive role for the emission of X-rays. With decreasing Z, a trend to lower skin dose rates was found for tungsten (Z = 74), steel (Z = 26), aluminum alloy (Z = 13), and glass for equal laser and machining conditions (Legall et al., 2018). However, additional aspects also play a role, such

as heating phenomena at high pulse repetition rates and a pre-structuring of the sample surface that might result in deviations from the "*Z*-law" (Legall et al., 2019, Legall et al., 2020).

The conversion efficiency from laser light into X-ray photons normalized to the target atomic number *Z* scales with the laser wavelength λ and the laser intensity *I* according to $\lambda \times I^{0.5}$ (Yu et al., 1999). An increasing emission of X-rays with laser intensity was confirmed by several groups for ultra-short laser machining in air and peak intensities exceeding 10^{13} W/cm^2 (Legall et al., 2018, Weber et al., 2019, Freitag and Giedl-Wagner, 2020). Recently, the comparison of data of different groups for machining of tungsten and steel at laser wavelengths of 1030 nm and 515 nm showed a significantly lower emission of X-rays at 515 nm laser wavelength in comparison to 1030 nm (Legall et al., 2021).

It should be underlined here that the emission of X-rays results from a complex interplay of laser and material parameters and additionally the processing conditions. As an example, the intra-line pulse separation (i.e. the spatial displacement of consecutive laser pulses (spots) at the sample surface) and the direction of the laser beam polarization with respect to the scanning direction influence the X-ray dose for a beam scanning regime (Legall et al., 2019).

4. X-ray spectra

The detailed knowledge of the spectral distribution of the X-ray emission during laser materials processing is required to calculate a proper radiation shielding to fulfill the requirements of regulatory radiation protection. Spectral measurements of pulsed X-ray radiation can be performed e.g. with TLD-based few-channel spectrometers and with semiconductor detectors in the single pulse mode. While the few-channel spectrometer is traceable to German national radiation standards (PTB), a detection sensitivity of almost 100% over an energy range of 6-60 keV can be realized with CdTe detectors. Even though the TLD-based measurement is extremely reliable for pulsed X-rays, a disadvantage of TLD-based spectrometers is their complex handling and a sophisticated data evaluation procedure. A problem that must be considered when using CdTe detectors is the appearance of the so-called *pile-up*. Pile-up occurs when two X-ray photons hit the detector simultaneously and are interpreted as a single photon with the sum of the energies of the individual photons. The pile-up effect can be strongly reduced by attenuating the incident radiation field to a certain limit. The fact that no pile-up can emerge up to twice the lowest photon energy incident on the detector allows to establish a simple method for pile-up free measurements. For this purpose, a series of X-ray spectra with increasing filter thickness is recorded. Thereby, the energy range of the radiation field incident on the detector is restricted by increasing the lowest detectable X-ray photon energy. From the pile-up-free regions of these successively measured spectra, a pile-up-free total spectrum can then be assembled over the whole energy range. If in addition, the measurements are performed at large distances from the X-ray source, the pile-up-free spectral ranges of each sub-spectrum can be further extended. The procedure is illustrated in Fig. 2. Here, the energy range <5 keV was theoretically extrapolated using a Maxwell-Boltzmann distribution.

Figure 3 shows a comparison of spectra reached with CdTe detector (BAM) and TLD-based few-channel spectrometer measurements (Behrens et al., 2019) for 100 mm distance to the laser-irradiation spot in all cases, respectively. The laser parameters were comparable in both measurements, however, the process management for the treatment of tungsten and a tungsten alloy was different. All X-ray spectra show significant contributions >5 keV.

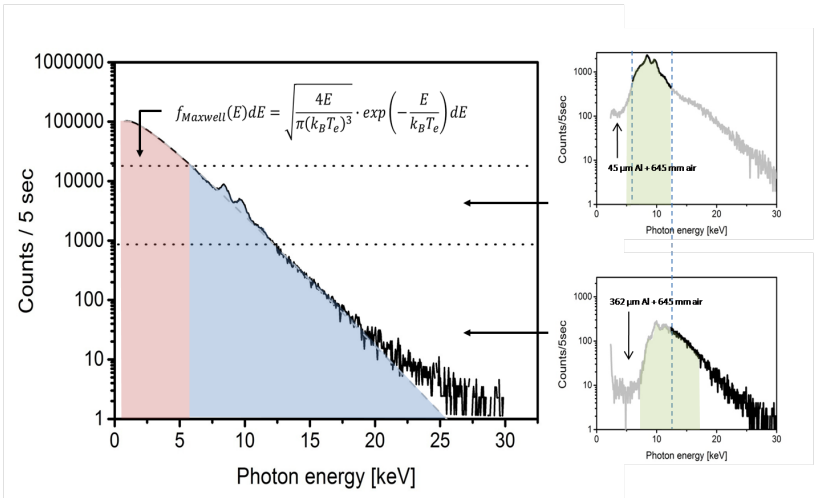

Fig. 2. Total X-ray emission spectrum in vacuum (left), constructed from two measured X-ray emission spectra in air (right). The measurements at a distance of 645 mm in air were performed with tungsten as target material at a peak intensity of 2.6×10^{14} W/cm^2 (1030 nm wavelength, 925 fs pulse duration). The upper spectrum at the right is attenuated by a 45 µm thick aluminum foil, the lower spectrum by a 362 µm thick aluminum foil. The total spectrum was extrapolated to lower X-ray photon energies by a Maxwellian distribution f_{Maxwell} (grey dashed line). E denotes the X-ray photon energy, k_B is the Boltzmann constant, and T_e is the electron temperature.

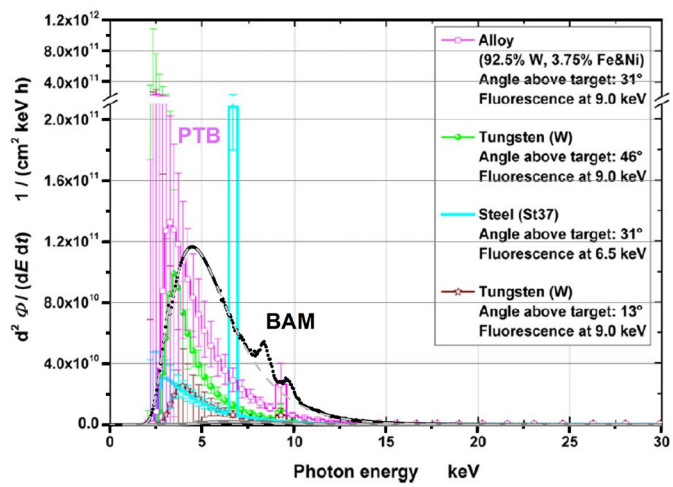

Fig. 3. X-ray flux (Φ) spectra calculated from measurements in air at a peak intensity of 2.1×10^{14} W/cm^2 performed with a TLD-based few channel spectrometer (normalized to the effective irradiation time and 100 mm distance). The uncertainty bars represent the 95% coverage intervals. Note that the ordinate is broken and has a 10-times larger scale. Pink curve (PTB): Tungsten alloy at an angle to the target surface of 31° (Data from Behrens et al., 2019). Black curve (BAM): Spectral X-ray photon fluence for tungsten calculated from measured spectra with a CdTe-spectrometer in air at an angle to the target surface of 29° and a peak intensity of 2.6×10^{14} W/cm^2 at 100 mm distance to the ablation spot. Additionally, the photon flux calculated from a Maxwell-Boltzmann distribution is shown (grey dashed line). The photon numbers of both spectra (PTB and BAM) are comparable.

5. Radiation protection shielding

Once the spectral X-ray emission from a laser processing system has been determined, an appropriate radiation shielding can be calculated for protection. For this purpose, the radiation field incident on the shielding material is multiplied by the spectral transmission of the chosen shielding material (Henke et al., 1993). The resulting X-ray dose behind the shielding can be calculated from the X-ray spectrum behind the shielding using conversion factors provided by the ICRU (ICRU, 1998) or by other sources (Veinot and Hertel, 2011). With this procedure, a shield of 1 mm steel was identified to meet the regulatory ambient dose of 1 µSv/h at a distance of 10 cm from the touchable surface of the shielding material for a laser pulse duration of ~1 ps, at a laser wavelength of 1030 nm, a pulse repetition rate of 400 kHz, and a peak intensity of 2.6×10^{14} W/cm^2. In this conservative estimation, the thickness of the radiation protection material was multiplied by a factor of two in order to meet the requirements with certainty even for deviating X-ray emission characteristics e.g. due to other process parameters or a different characteristic of the laser field.

Acknowledgements

The authors gratefully acknowledge financial support by the German Federal Ministry of Education and Research (BMBF) in the funding program Photonics Research Germany under contract number 13N14249 and the Federal Office for Radiation Protection (BfS) for the support under the administrative agreement with contract number 3619S22370.

References

Alves, J.G., Ambrosi, P., Bartlett, D.T., Currivan, L., van Dijk, J.W.E., Fantuzzi, E., Kamenopoulou, V. 2011. The new EC technical recommendations for monitoring individuals occupationally exposed to external radiation. Radiation Protection Dosimetry 144, p. 17.

Behrens, R., Pullner, B., Reginatto, M. 2019. X-ray emission from materials processing lasers. Radiation Protection Dosimetry 183, p. 361.

Freitag, C., Giedl-Wagner, R. 2020. X-ray protection in an industrial production environment. PhotonicsViews 3, p. 37.

Henke, B.L., Gullikson, E.M., Davis, J.C. 1993. X-ray interactions: photoabsorption, scattering, transmission, and reflection at E=50-30000 eV, Z=1-92. Atomic Data and Nuclear Data Tables 54, p. 181.

ICRU. 1998. International Commission on Radiation Units and Measurements (ICRU). Conversion coefficients for use in radiological protection against external radiation. ICRU report 57.

Legall, H., Schwanke, C., Pentzien, S. , Dittmar, G., Bonse, J., Krüger, J. 2018. X-ray emission as a potential hazard during ultrashort pulse laser material processing. Applied Physics A 124, p. 407.

Legall, H., Schwanke, C., Bonse, J., Krüger, J. 2019. The influence of processing parameters on X-ray emission during ultra-short pulse laser machining. Applied Physics A 125, p. 570.

Legall, H., Schwanke, C., Bonse, J., Krüger, J. 2019a. X-ray emission during ultrashort pulse laser processing. Proc. of SPIE 10908, p. 1090802.

Legall, H., Schwanke, C., Bonse, J., Krüger, J. 2020. X-ray radiation protection aspects during ultrashort laser processing. Journal of Laser Applications 32, p. 022004.

Legall, H., Bonse, J., Krüger, J. 2021. Review of X-ray exposure and safety issues arising from ultra-short pulse laser material processing. Journal of Radiological Protection 41, p. R28.

Weber, R., Giedl-Wagner, R., Förster, D.J., Pauli, A., Graf, T., Balmer, J.E. 2019. Expected X-ray dose rates resulting from industrial ultrafast laser applications. Applied Physics A 125, p. 635.

Veinot, K.G., Hertel, N.E. 2011. Personal dose equivalent conversion coefficients for photons to 1 GeV. Radiation Protection Dosimetry 145, p. 28.

Yu, J., Jiang, Z., Kieffer, J.C., Krol, A. 1999. Hard X-ray emission in high intensity femtosecond laser–target interaction. Physics of Plasmas 6, p. 1318.